Front. Optoelectron. 2019, 12(1): 41–51
https://doi.org/10.1007/s12200-018-0836-7

REVIEW ARTICLE

Vector mode based optical direct detection orthogonal frequency division multiplexing transmission in short-reach optical link

Jianping LI[1], Zhaohui LI (✉)[2]

1 Guangdong Provincial Key Laboratory of Optical Fiber Sensing and Communications, Institute of Photonics Technology, Jinan University, Guangzhou 510632, China
2 State Key Laboratory of Optoelectronic Materials and Technologies and School of Electronics and Information Technology, Sun Yat-sen University, Guangzhou 510275, China

Abstract As one solution to implement the large-capacity space division multiplexing (SDM) transmission systems, the mode division multiplexing (MDM) has gained much attention recently. The vector mode (VM), which is the eigenmode of the optical fiber, has also been adopted to realize the optical communications including the transmission over free-space optical (FSO) and optical fiber links. Considering the concerns on the short-reach optical interconnects, the low cost and high integration technologies should be developed. Direct detection (DD) with higher-order modulation formats in combination of MDM technologies could offer an available trade-off in system performance and complexity. We review demonstrations of FSO and fiber high-speed data transmission based on the VM MDM (VMDM) technologies. The special VMs, cylindrical vector beams (CVB), have been generated by the *q*-plate (QP) and characterized accordingly. And then they were used to implement the VMDM transmission with direct-detection orthogonal frequency division multiplexing (DD-OFDM). These demonstrations show the potential of VMDM-DD-OFDM technology in the large-capacity short-reach transmission links.

Keywords space division multiplexing (SDM), mode division multiplexing (MDM), few-mode fiber (FMF), vector mode (VM), cylindrical vector beam (CVB), orthogonal frequency division multiplexing (OFDM), direct detection (DD), optical interconnect

Received May 30, 2018; accepted July 9, 2018

E-mail: lzhh88@sysu.edu.cn

Invited Paper

1 Introduction

The rapid increasing demand for data traffic coming from the Internet of Things (IOT), cloud services, online game, video and business etc., is driving the modern optical communication systems, including the short-reach optical interconnect systems, to increase the transmission data rate and capacity timely [1]. In general, there are technologically numerous methods to meet the bandwidth and density requirements of short-reach datacenter optical interconnect. Under the consideration of the most important concerns of low cost and high integration on the short reach optical interconnection systems, the optical spatial division multiplexing (SDM), which is regarded as the last unexplored physical dimension to improve the capacity of optical communication [2–4], has been studied recently. And the SDM-based architecture could provide best cost-performance tradeoff depend on the network load and data center (DC) size [5].

SDM-based technologies are involved the use of fiber bundle with multiple parallel optical fibers together, coupled or uncoupled multi-core fiber (MCF), and few-mode or multi-mode fiber (FMF/MMF). The later one is also categorized as the mode division multiplexing (MDM) technology because the multiple orthogonal fiber modes are used as the individual channels to transmit optical signal. MDM technique has been demonstrated in short-reach optical interconnects by means of mode-group (MG) multiplexing [6,7], linearly polarized modes (LPMs) multiplexing [8,9], orbital angular momentum (OAM) multiplexing [10–12], and vector modes (VMs) multiplexing [13–16]. In general, VMs are the eigenmodes supported by the optical fiber with spatially inhommogeous states of polarization (SOP). As one kind of VMs,

the cylindrical vector beams (CVBs), whose SOP is cylindrically symmetric, has been studied in various research fields. But, the data transmission based on VM over optical fiber has not been demonstrated widely so far. Recently, 4 × 10 Gb/s CVB-based (the order of ±2) multiplexing transmission with the on-off keying (OOK) signal over 5-km link FMF has been demonstrated [17]. Researchers also use compact, integrated optics to realize the 2 × 20 Gb/s eigenmode multiplexing communication in 2-km circular optical fiber [18]. However, most of these newly employed MDM transmissions are based on the coherent detection which is not the best choice for the short-reach optical interconnects.

In this paper, we review the demonstrations of VM-based MDM (VMDM in briefly) transmission over free-space optical link and 4-mode FMF with the aim to improve the data rate and transmission capacity. The beam quality of VM generated using *q*-plate (QP) as well as the induced mode crosstalk have been analyzed. And the VMDM transmissions have been demonstrated by using the modulation of direct-detection (DD) orthogonal-frequency-division-multiplexing (OFDM) without multiple-input multiple-output (MIMO) digital signal processing (DSP).

In Section 2, we discuss the VM generation and characterization used in VMDM transmission systems. We introduce the QPs that used to realize the basic CVBs (TE and TM modes) generation and higher-order mode conversion based on conventional phase plates. In Section 3, we describe the VMDM transmission experiments in free-space optical link with DD-OFDM modulation. The demonstrations have been implemented for a two-mode 120 Gb/s quadrature phase shift keying (QPSK) transmission over 80 cm and a four-mode 95.16 Gb/s transmission over 20 cm respectively with direct detection. In Section 4, we show the transmission experiment performed on a four-mode FMF supporting four linearly polarized modes which correspond to seven fiber vector eigenmodes. A modal decomposition scheme based on polarization grating is used to analyze the mode inter-coupling and the variation of spatial and polarization distribution when the CVBs propagate in the few-mode fiber. By using the eigenmode of TM_{01} and TE_{01}, the 95.16 Gb/s over 5 m four-mode FMF and 47.58 Gb/s over 10 0m four-mode FMF transmissions have been realized with the DD-OFDM technology. Note that there is no MIMO processing in these vector-mode-based demonstrations. Finally, the conclusions are made in the end of the paper.

2 Vector mode generation and characterization

Like the other MDM transmission systems, the mode converter used to realize the VM generation in the VMDM-DD-OFDM system is also one kind of the key components. Currently, many methods including fiber-based and liquid-crystal-based can be used to realize VM conversion. Here we describe the QPs which are passive liquid crystal optical devices used as the mode converter. QP can change the spatial distribution of the SOP of a homogenous polarized optical field. To perform the VMDM-DD-OFDM transmission, the properties of the used QP should be measured first. And then, the characterization of the generated VMs has been implemented subsequently.

2.1 Properties measurement of *q*-plates

In general, the optical axis orientation α of QP in the *x*-*y* plane can be assumed to be given as follows

$$\alpha(r,\varphi) = q\varphi + \alpha_0, \tag{1}$$

where (r, φ) stands for the points on the transverse plane. q is the topological charge and α_0 a constant offset angle. Here, the QPs with q = 1/2 fabricated by Arcoptix company are used to do the demonstration. The Jones matrix of QP can be described as $\boldsymbol{J}_s$ [19]

$$\begin{aligned}\boldsymbol{J}_s &= \begin{bmatrix} \cos 2\alpha & \sin 2\alpha \\ \sin 2\alpha & -\cos 2\alpha \end{bmatrix} \\ &= \begin{bmatrix} \cos 2(q\varphi+\alpha_0) & \sin 2(q\varphi+\alpha_0) \\ \sin 2(q\varphi+\alpha_0) & -\cos 2(q\varphi+\alpha_0) \end{bmatrix}. \end{aligned} \tag{2}$$

The output optical-field of a linearly polarized light after passing through the QP can be expressed as $\boldsymbol{E}_{out} = \boldsymbol{J}_s\boldsymbol{E}_{in}$. Then the different polarization patterns can be obtained. Figure 1(a) shows the schematic diagram of the QPs characterization. The wavelength and power of the input continuous-wave (CW) light are about 1549.994 nm and power of 12.5 dBm respectively. Then the light is collimated by the lens (L), fed into the QP to realize the VM conversion after filtered by the linear polarizer (LP), and detected by (i) the spatial optical power meter (SOPM) and (ii) common OPM respectively. At the same time, the charge-coupled device (CCD) camera (iii) is used to capture the intensity profiles of generated VMs [14].

The measured power of QPs by SOPM (i) and OPM (ii) have been shown in Figs. 1(b) and 1(c), respectively. Obviously, the performances of QPs have a good agreement with each other. The QP insertion loss is around 5 dB. But, the optical power shows an abrupt variation when $V_b > 1.2$ V. This meant that a large portion of input laser has not been converted to the VMs. The insets show the captured intensity profiles when V_b equaling to 0.1, 2.0 and 4.2 V respectively. It can be observed that the higher-order VMs can be realized under the regular operation region (ROR), while no VM can be

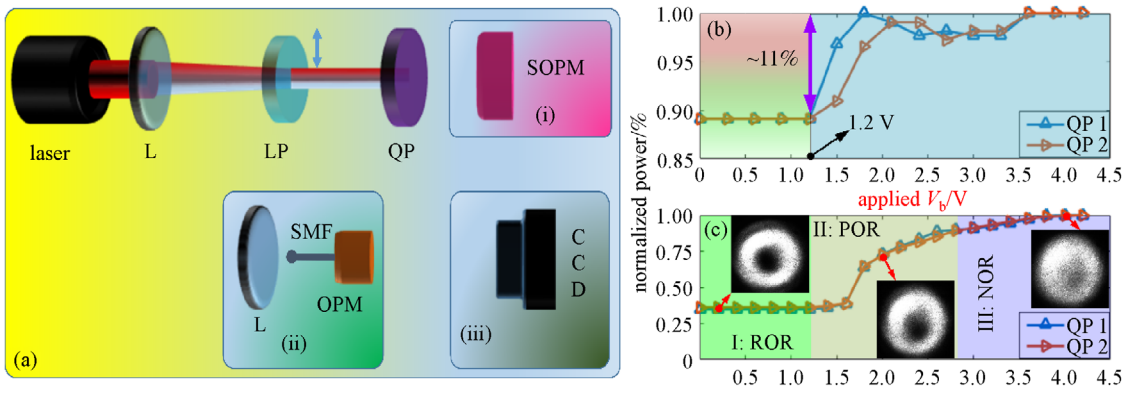

Fig. 1 (a) Schematic setup for q-plate (QP) characterization by using (i) spatial optical power meter (SOPM), (ii) common OPM, and (iii) charged-coupled device (CCD) camera. L: lens; LP: linear polarizer. And the normalized power vs. applied V_b based on (b) SOPM and (c) OPM. ROR: regular operational region; POR: partial operational region and NOR: non-operational region [14]

generated within the non-operational region (NOR). As a result, a few VMs with lower pureness will be found when V_b biased in the partial operational region (POR).

2.2 Vector mode generation and characterization

2.2.1 TE_{01} and TM_{01} modes characterization

The characterization of VMs generated by the two QPs is shown as follows. With the use of Jones vector, the SOP of VMs can be expressed as [19]

$$|l,\gamma\rangle = [\cos(l\varphi+\gamma) \quad \sin(l\varphi+\gamma)]^{\mathrm{T}}, \tag{3}$$

where $l = \pm1,\pm2,\ldots$, and $\gamma = 0, \pi/2$. For example, Jones vector $(\cos\varphi \ \sin\varphi)^{\mathrm{T}}$ and $(-\sin\varphi \ \cos\varphi)^{\mathrm{T}}$ stand for the radially (TM_{01} mode) and azimuthally (TE_{01} mode) polarized optical fields, respectively. These two typical VMs can be generated by QPs with proper bias voltage. To characterize them, the intensity profiles captured by CCD camera are used to identify the polarization distribution with rotating the LP to a specific angle. The bias voltage V_b was set to 0 V based on the previous measurement. The characterization results of the generated TE_{01} and TM_{01} modes are shown in Fig. 2. A rotation of ~ 45° of the direction can be observed that would be induced by the constant offset α_0 of QPs. In addition, the crosstalk between the two CVBs has been measured in terms of a mode isolation (MI) which is > 20 dB.

2.2.2 Higher-order vector modes characterization

Besides the basic 1st-order eigenmodes of TE_{01} and TM_{01}, there are other CVB modes, such as HE_{21e} and HE_{21o} modes, can be used to build the VMDM systems. Here, we perform the arbitrary VM conversion by using a few *q*-plate (QPs) and half-wave plates (HWPs).

The higher-order Poincaré sphere model based VM transformations have been shown in Fig. 3 [20]. θ and ϕ are the colatitude and azimuth angles over the sphere ($\theta \in [0, \pi]$, $\phi \in [0, 2\pi]$). Then, an arbitrary SOP $\Psi_l|\theta,\phi\rangle$ can be described as below

$$\Psi_l|\theta,\phi\rangle = \cos\left(\frac{\theta}{2}\right)|L_l\rangle e^{\frac{i\phi}{2}} + \sin\left(\frac{\theta}{2}\right)|R_l\rangle e^{-\frac{i\phi}{2}}, \tag{4}$$

where $|L_l\rangle = (\hat{x}+i\hat{y})e^{-il\varphi}/\sqrt{2}$ and $|R_l\rangle = (\hat{x}-i\hat{y})e^{il\varphi}/\sqrt{2}$ represent left and right-circular polarized components

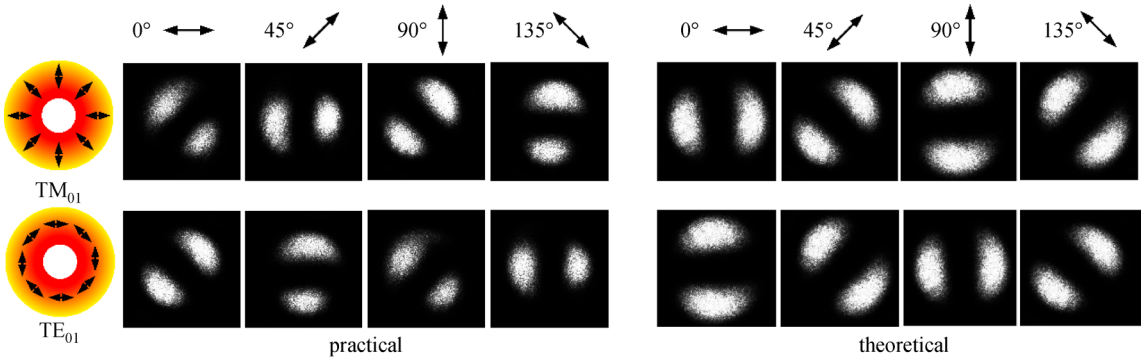

Fig. 2 Experiment results of VM characterization [14]

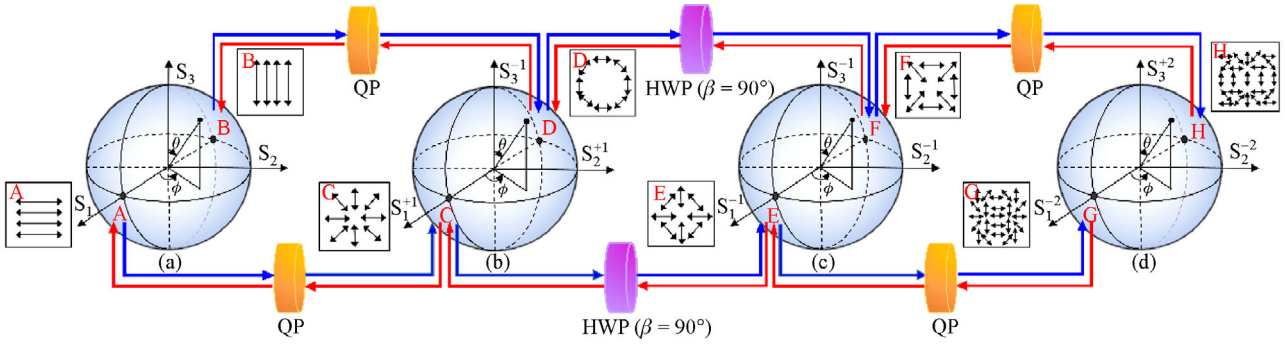

Fig. 3 Typical Poincaré spheres for (a) l = 0, (b) l = 1, (c) l = – 1 and (d) l = 2 respectively [20]

corresponding to north and south poles on the sphere, respectively. l and φ are the order and azimuthal angle of Poincaré spheres. The point located at equators in Figs. 3(b), 3(c) and 3(d) stand for the SOPs with inhomogeneous linear polarization. Then these SOPs can be described as below

$$\Psi_l|\frac{\pi}{2},\phi\rangle = \left[\cos\left(\frac{\phi}{2}-l\varphi\right)-\sin\left(\frac{\phi}{2}-l\varphi\right)\right]^{\mathrm{T}}. \quad (5)$$

Thus, C $(\cos\varphi \ \ \sin\varphi)^{\mathrm{T}}$ and D $(\sin\varphi \ -\cos\varphi)^{\mathrm{T}}$ shown in Fig. 3(b) stand for the radial and azimuthal CVB modes, respectively. Except for C and D, the other points of the equator stand for the generalized CVB modes which are a linear superposition of them. With the assumption of α_0 = 0, the general transformation of VMs can be described as below

$$\begin{aligned}\Psi_l|\frac{\pi}{2},\phi\rangle &\overset{\mathrm{QP}\ (\alpha_0=0)}{\Longleftrightarrow} \Psi_{(2q-l)}|\frac{\pi}{2},-\phi\rangle,\\ \Psi_l|\frac{\pi}{2},\phi\rangle &\overset{\mathrm{HWP}}{\Longleftrightarrow} \Psi_{-l}|\frac{\pi}{2},-(\phi+4\alpha)\rangle.\end{aligned} \quad (6)$$

The experimental used to validate CVB mode conversion is illustrated in Fig. 4. Here, the beam waist of input laser source (λ = 1550 nm, power = 12.5 dBm) is collimated to ~2.1 mm before passing the linear polarizer.

Figure 5$(A_1)/(A_2)-(E_1)/(E_2)$ show the intensity profiles at the different locations (A, B, C, D and E) labeled in Fig. 4. The TM_{01}/TE_{01} modes are first converted by QP1 following an HWP1 with fast axis at $\pi/2$, and subsequently transformed into HE_{21e}/HE_{21o} modes. The inset 4(i) is used to show the inverse process of Eq. (6). Namely, HE_{21e}/HE_{21o} modes will be converted to TM_{01}/TE_{01} modes by HWP2. Accordingly, inset 4(ii) shows that HE_{21e}/HE_{21o} modes will be transformed to higher-order VMs if HWP2 was replaced with QP2. Figure 5$(b_1)/(b_2)-(e_1)/(e_2)$ depict the SOPs of the four typical CVBs. Thus, the demonstration shows that the various VMs have been effectively converted by using the simple setup.

Figure 6 indicates the experimental results of modal isolation among these VMs. It can be observed that a maximum MI of – 10.3 dB between these mode channels induced by the QPs and other impact factors.

3 VMDM-DD-OFDM transmission in free-space optical link

In this section, we perform the high-speed VMDM-based free-space optical (FSO) transmission with high-order modulation formats.

3.1 Two-mode VMDM transmission

The demonstration of two-mode VMDM transmission is shown in Fig. 7 [14]. The wavelength, linewidth and power of the used external cavity laser (ECL) at the transmitter are 1549.994 nm, < 100 kHz and 14.5 dBm respectively. An arbitrary waveform generator (AWG, Tektronix AWG 70002A) with a 25 Gs/s sampling rate is used to generate the electrical OFDM signal of V_{pp} ((peak-to-peak voltage) ~ 1 V. Then, an intensity modulator (IM, Photoline MX-

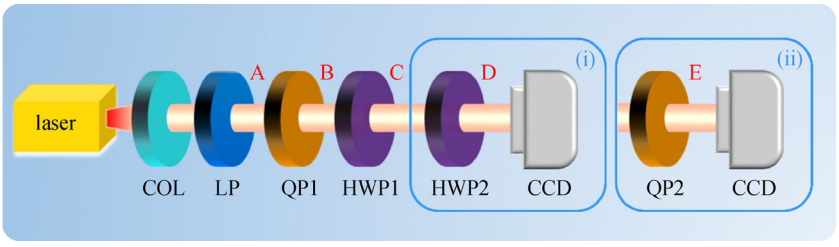

Fig. 4 Schematic of effective conversion between different VMs. COL: collimator [20]

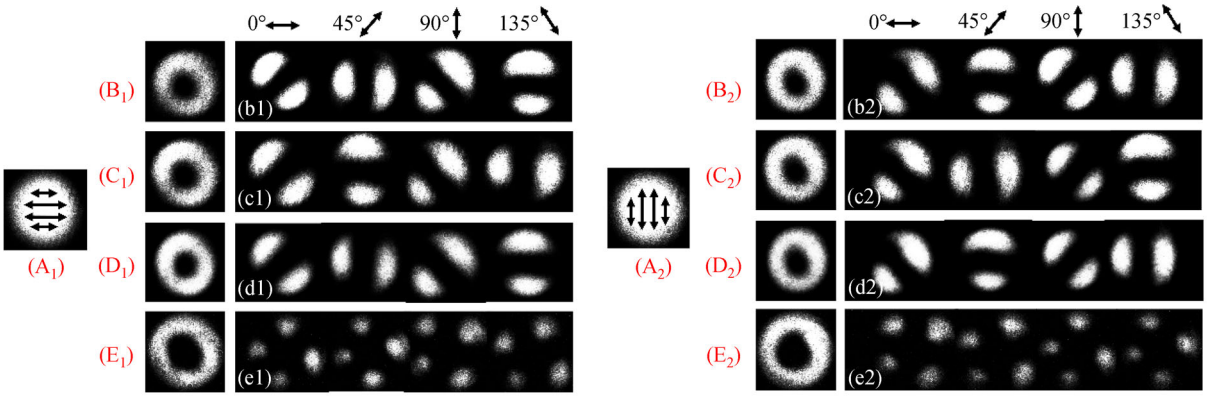

Fig. 5 Insets $(A_1)/(A_2)$–$(E_1)/(E_2)$ show the intensity profiles of typical VMs labeled in Fig. 4. Insets $(b_1)/(b_2)$–$(e_1)/(e_2)$ indicate the polarization distribution of the these VMs [20]

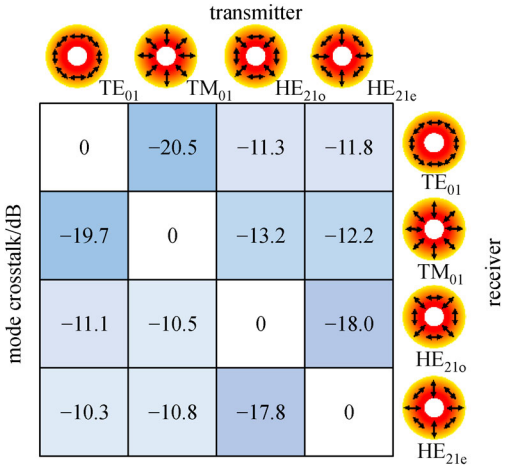

Fig. 6 Mode crosstalk of different VMs [20]

LN-40) with the half-wave voltage and bias voltage of 3.4 and 1.9 V respectively is used to realize the optical OFDM modulation before amplified by the EDFA1. Other parameters used in the experiment are can be found in Ref. [14]. After VM division multiplexing by QP1 and transmission over FSO link, the optical OFDM signal is mode de-multiplexed by QP2 and PBS. Insets (i)–(iv) show the intensity profiles of the points A, B, C and D labeled in Fig. 7. Then, the transmitted signal is pre-amplified by another Erbium-doped fiber amplifier (EDFA) and then filtered by a tunable optical filter (TOF). At optical receiver, a PD (u2t XPDV2120R, 3-dB bandwidth of 50 GHz) is used to realize the optical-to-electrical (O/E) conversion adjusted by a variable optical attenuator (VOA). Then the real-time oscilloscope (OSC, LecroyLab-Master 10-36Zi) is used to sample the yield electrical signal which would be processed off-line. And the electrical spectrum of this signal shown in inset (v).

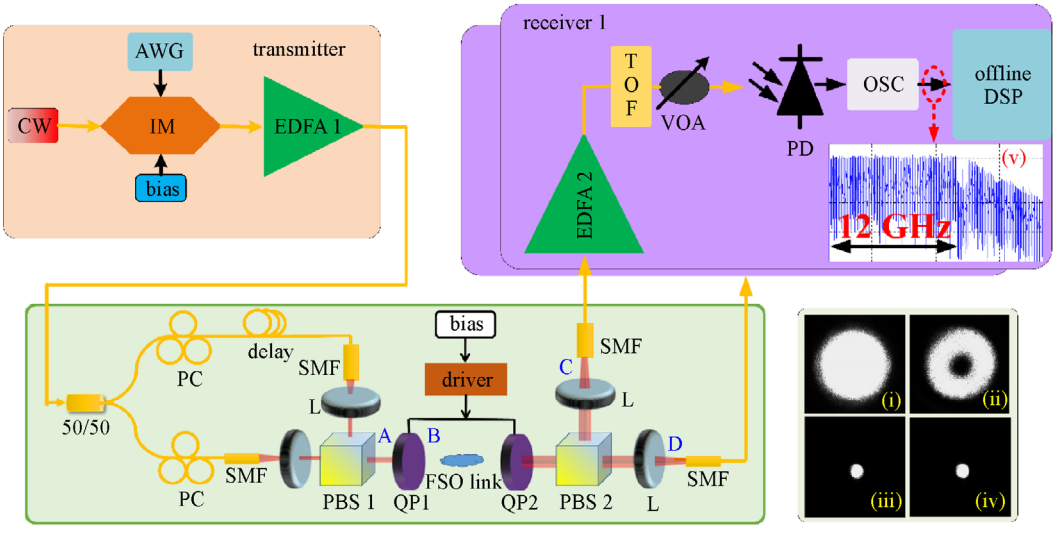

Fig. 7 Experimental setup for VMDM-based optical transmission in FSO link. IM: intensity modulator; AWG: arbitrary waveform generator; EDFA: Erbium-doped fiber amplifier; PC: polarization controller; SMF: single mode fiber; PBS: polarization beam splitter; TOF: tunable optical filter; VOA: variable optical attenuator; PD: photo-detector; OSC: oscilloscope [14]

Then the off-line digital signal processing (DSP) is used to further process the received signal. The total raw bit rate of this two-mode demonstrateion is 120.12 Gbit/s.

The measured bit-error-ratio (BER) performances are shown in Fig. 8(a). The power penalty between the single VM channel and "back to back" (B2B) transmission is found to be ~1.88 dB. And only 0.55 dB power penalty is induced when the two VMs are transmitted simultaneously. Figure 8(b) shows the constellations of the demodulated OFDM/32QAM signals corresponding to the cases shown in Fig. 8(a) with the received power of −14 dBm.

3.2 Four-mode VMDM transmission

The demonstration of four-mode VMDM-DD-OFDM transmission over FSO link is shown in Fig. 9 [20]. The basic configuration of the experiment is the same with Fig. 7 except the parts of generation and demodulation of the higher-order VMs. At transmitter, the optical carrier with wavelength of 1550 nm is modulated by a QPSK-OFDM signal generated as the same way in Section 3.1. After amplified by EDFA, the output optical signal is split into two branches via an optical coupler (OC) and then converted to TE_{01} and TM_{01} modes through QP1. Afterwards, the optical signals are split by a non-polarizing 50:50 beam splitters (NPBS). One part is converted into HE_{21e}/HE_{21o} with an HWP ($\beta=\pi/2$). Thereafter, four VMs have been combined by the other NPBS. According to the parameters in Ref. [20], the aggregate raw bit rate of this experiment is 95.16 Gb/s. The intensity profile of the multiplexed four VMs is shown in inset (a) of in Fig. 9.

At receiver side, VM demultiplexing is realized via two steps after ~ 20 cm FSO transmission. The first step, HWP2 ($\beta=\pi/2$) is used (dotted-rectangle in Fig. 9), HE_{21e}/HE_{21o} will be converted to the fundamental mode. Figure 9 (b) shows the intensity profile of the demultiplexed VMs. But, TE_{01} and TM_{01} modes will be converted to higher-order VMs which cannot be guided by SMF. Figure 9(c) shows the intensity profile of the un-demultiplexed higher-order VMs. The second step, HWP2 is removed from the optical path, only TE_{01} and TM_{01} modes will be demodulated. Figures 9(d) and 9(e) show the intensity profiles of the case respectively. Then PBS is used to split two demodulated channels.

The transmission performances are shown in Fig. 10(a). When the two channels of TE_{01} and TM_{01}, or HE_{21e}/HE_{21o} are propagated, power penalties of 0.8 and 0.75 dB, or 1.1 and 1.25 dB will be induced under the forward error correction (FEC) threshold of 3.8×10^{-3}. But, the power penalties will be 3.5, 3.35, 4.1 and 4.1 dB for TE_{01}, TM_{01}, HE_{21e}/HE_{21o} channels, respectively when they transmitted simultaneously.

3.3 Multichannel two-mode VMDM transmission

In this section, we shown the demonstration of VMDM in combination of wavelength division multiplexing (WDM) shown as in Fig. 11 [21]. At the transmitter, an optical frequency comb generator (OFCG) (OptoComb WTAS-02) is used to generate the desired multiple wavelengths with a wavelength interval of ~ 0.2 nm. A wavelength selective switch (WSS, Waveshaper 4000S) is used to shape the performance of the desired channels. The optical spectrum of the 20 WDM channels covering 4 nm range is shown in inset (ii).

Like the same procedure implemented in the previous experiment, after amplified by an EDFA, the optical carriers are launched into the IM and modulated by a QPSK-OFDM signal generated by the AWG. Then the optical beam is split into two parts with an OC and combined by a PBS to realize the TE_{01} (Ch1) and TM_{01} modes (Ch2) conversion via QP, respectively.

The mode crosstalk of two VMs at five different wavelengths (within the range from 1548 to 1552 nm) are shown in Fig. 12(a). It can be observed that the

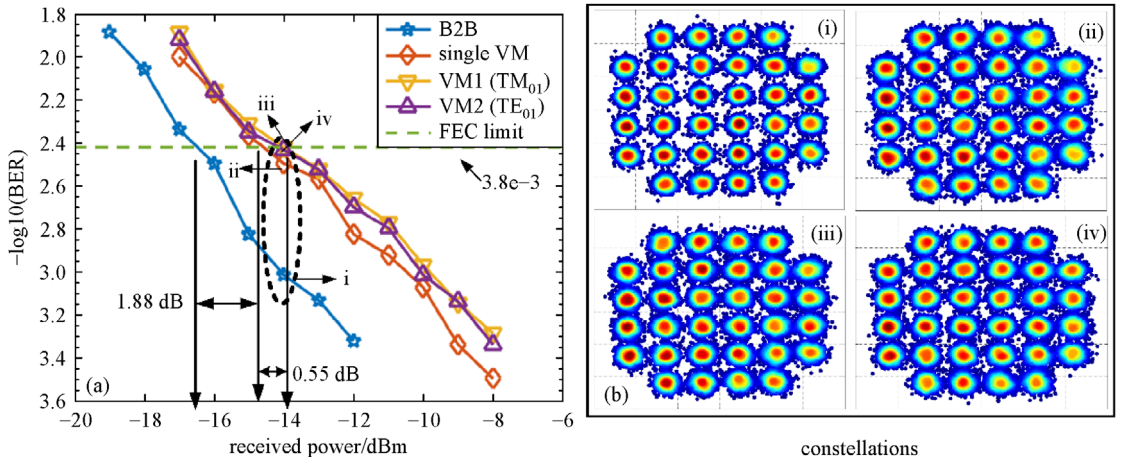

Fig. 8 (a) Bit-error-ratio (BER) performance of the two-mode VMDM transmission. B2B: back-to-back; (b) constellations for the cases (i, ii, iii and iv) dotted-circle in Fig. 7 when the received optical power is −14 dBm [14]

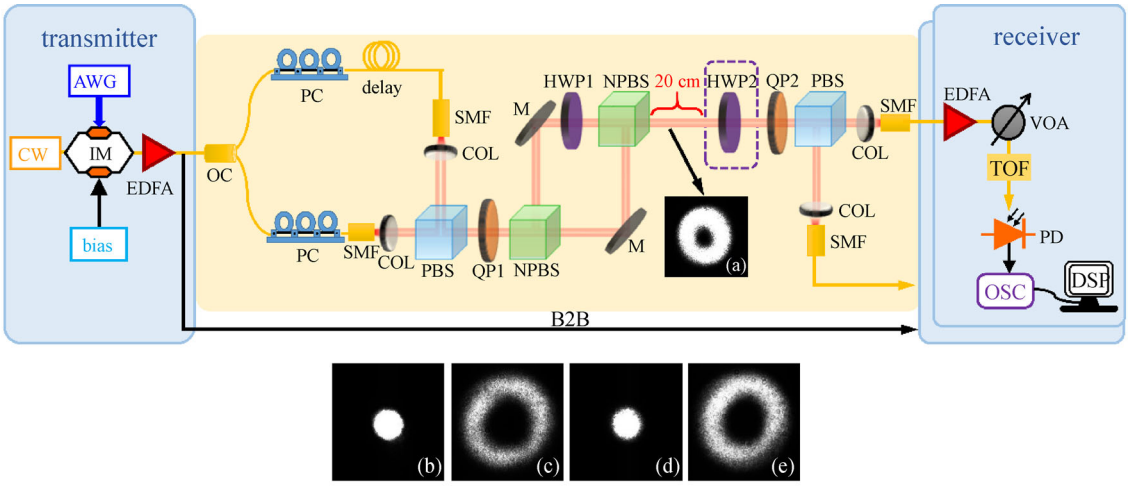

Fig. 9 Schematic of four-mode VMDM demonstration. Intensity profiles of (a) the 4 multiplexed VMs, (b) the demultiplexed HE_{21e} and HE_{21o} channels, (c) the un-demultiplexed TE_{01} and TM_{01} modes, (d) the demultiplexed VMs of TE_{01} and TM_{01} modes, and (e) the un-demultiplexed HE_{21e} and HE_{21o} modes [20]

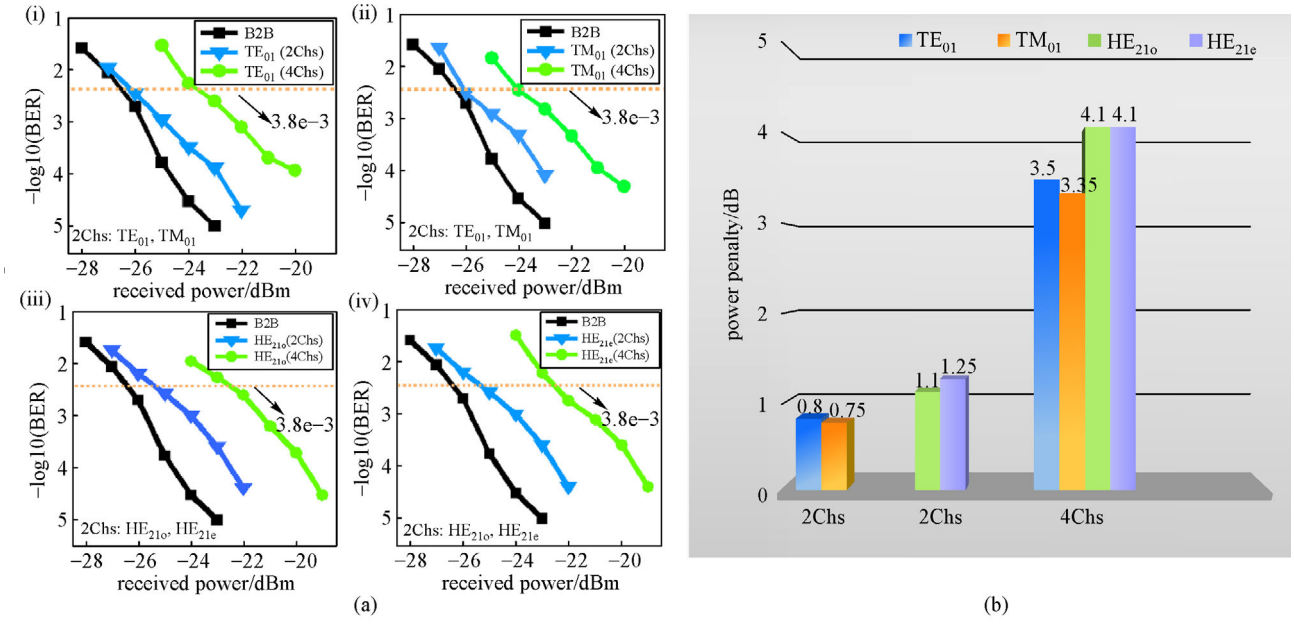

Fig. 10 (a) BER performance of VMDM transmission with 2 channels (2Chs) and 4 channels (4Chs), respectively; (b) power penalties for the cases shown in Fig. 10(a) [20]

maximum MI is around −17 dB between 2 channels. Figure 12(b) shows the measured BER performances. Obviously, the multichannel error-free transmission has realized under the FEC limit of 3.8×10^{-3}.

4 DD-OFDM transmission in few-mode fiber link

In principle, the VMs are the eigenmode of the optical fiber and can be converted using the fiber-based devices and then propagated through optical fibers with good performance [22]. Thus, we perform the extension of VMDM-DD-OFDM transmission over the few-mode fiber link [23]. According to the property of VM, a non-separable coupling will be involved in between the spatial and polarization degrees of freedom. This coupling will induce the mode crosstalk between different VMs. To analyze the crosstalk, we first perform the mode performance characterization.

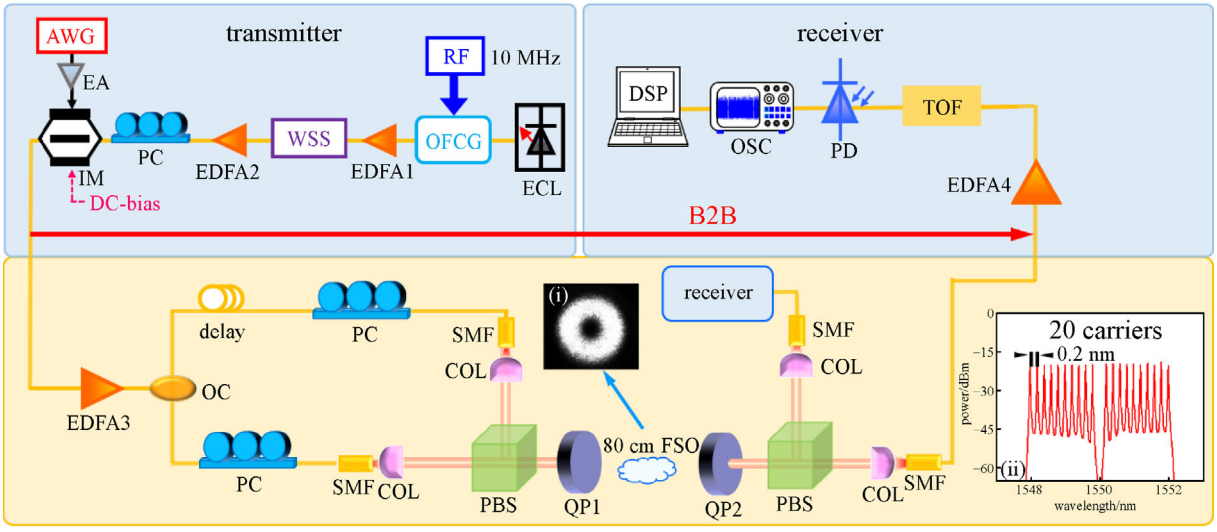

Fig. 11 Demonstration of multichannel VMDM transmission. OFCG: optical frequency comb generator; RF: ratio frequency; WSS: wavelength selective switch; EA: electrical amplifier. (i) Intensity profile of two multiplexed VMs, (ii) spectrum of OFCG after shaping by the WSS [21]

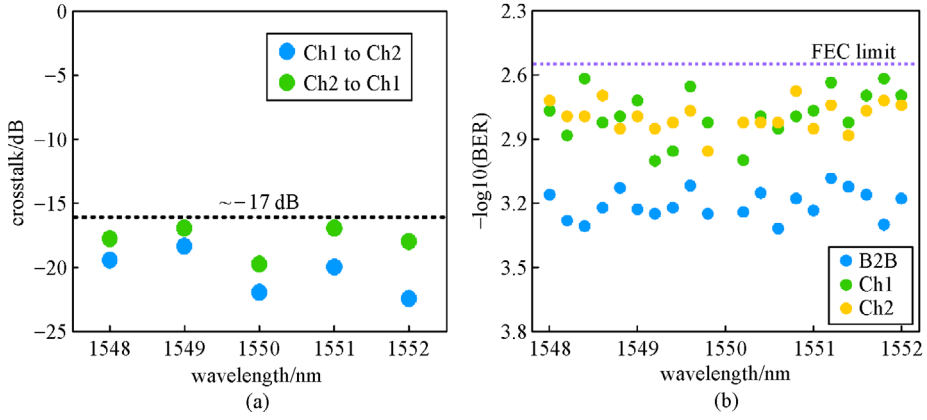

Fig. 12 (a) Measured crosstalk; (b) BER performances [21]

4.1 Crosstalk measurement during fiber propagation

Figure 13(a) shows the schematic of CVB mode performance characterization. As described in previous sections, the radially polarized VM TM_{01} (inset (i)) has been converted by QP and then launched into the 4-mode FMF link. Figure 13(d) shows the index profile of the used 4-mode FMF with a core diameter of 9.5 μm, a cladding diameter of 125 μm. Meanwhile, the index of the fiber core and cladding are 1.449 and 1.444 respectively. Thus, the VMs of HE_{11}, TE_{01}, TM_{01}, HE_{21}, HE_{12}, EH_{11} and HE_{31} at 1550 nm wavelength can be guided by the FMF. The polarization grating (PG) is used to split the two basic states with the opposite order from the output beams. To illustrate the influence of the non-separable coupling, we take the characterization of TM_{01} mode as an example. According to Eq. (4), a pure TM_{01} mode can be generated if the I_L and I_R part have the same scale. The respective power in different cases of transmission have been measured as shown in Fig. 13(b). It can be observed that the pureness of the TM_{01} mode is not very high. Therefore, the scale of the two components of TM_{01} mode becomes further imbalanced after transmission over the FMF. Figures 13(c)-(ii) and 13(c)-(iii) show the intensity profiles of two parts after transmission over 5 m FMF. At last, we use a quarter-wave plate (QWP) to compete the interference with Gaussian beam. These interference patterns have been shown in Figs. 13(c)-(iv) and 13(c)-(v).

The measured modal isolation between CVBs channels (TE_{01} and TM_{01}) is shown in Table 1, in which the respective minimum MIs are about 16.8 dB after transmitting over 5 m FMF and 12.5 dB over 100 m FMF. Based on the MI results, the VMDM-DD-OFDM transmissions over FMF link with different distance and modulation formats have been performed respectively.

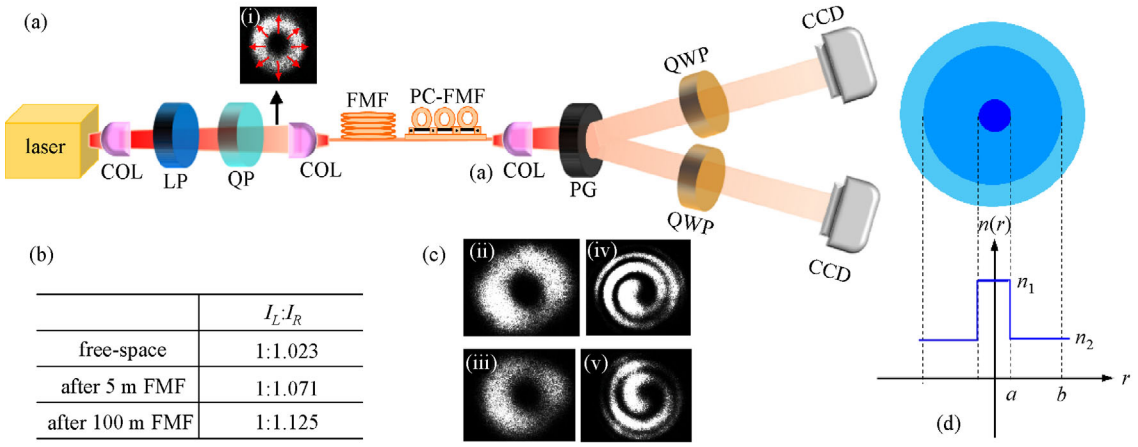

	I_L:I_R
free-space	1:1.023
after 5 m FMF	1:1.071
after 100 m FMF	1:1.125

Fig. 13 (a) Experiment setup for CVB performance characterization. FMF: four-mode few-mode fiber; PC-FMF: polarization controller fabricated by four-mode fiber; PG: polarization grating; QWP: quarter-wave plate. (i) Intensity profile of converted VM by QP. (b) Power ratio between the two basic states with transmission over different distances. (c) (ii) and (iii) are the intensity profiles of the two orthogonal states after 5 m FMF propagation; (iv) and (v) the interference patterns corresponding to the (ii) and (iii), respectively. (d) Index profile of the used FMF

Table 1 Modal isolation (dB) for CVBs transmission over the used FMF.

vector modes	5 m FMF		100 m FMF	
	TE_{01}	TM_{01}	TE_{01}	TM_{01}
TE_{01}	0	18.5	0	13.7
TM_{01}	16.8	0	12.5	0

4.2 Two-mode VMDM transmission

We perform the VMDM-DD-OFDM transmission over FMF link shown in Fig. 14 [23]. The ECL (1550 nm, 16 dBm) at transmitter is launched into an intensity modulator to realize the QPSK-OFDM signal modulation as abovementioned. The process of signal generation and mode conversion are the same as the previous sections. The intensity profiles of the fundamental mode and CVBs are shown in insets (i) and (ii). And a PC-FMF is adopted to adjust the polarization and intensity pattern of the channels at the end of the FMF. For instance, inset (iii) shows the intensity pattern after transmission over 100 m FMF. Then, the output beams are converted to the fundamental mode via QP2 as shown in inset (iv). At last, the two orthogonal mode channels are separated by the PBS. Similarly, the optical signals are received by a

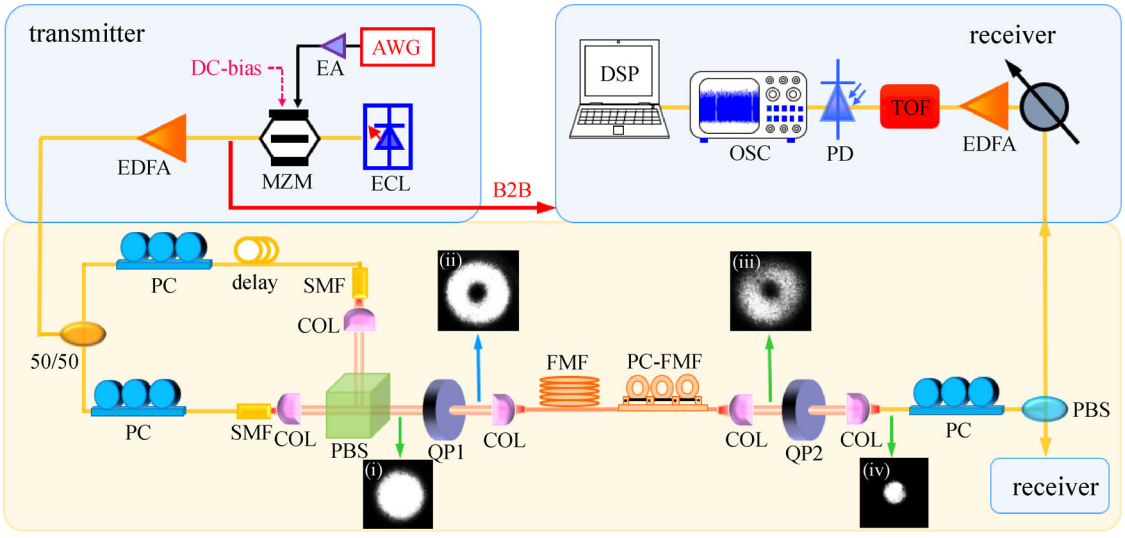

Fig. 14 Demonstrations of VMDM-DD-OFDM transmission over FMF link. Intensity profiles: (i) the unconverted fundamental mode, (ii) the converted CVBs, (iii) output CVBs after transmission 100 m FMF, and (iv) the de-multiplexed CVBs [23]

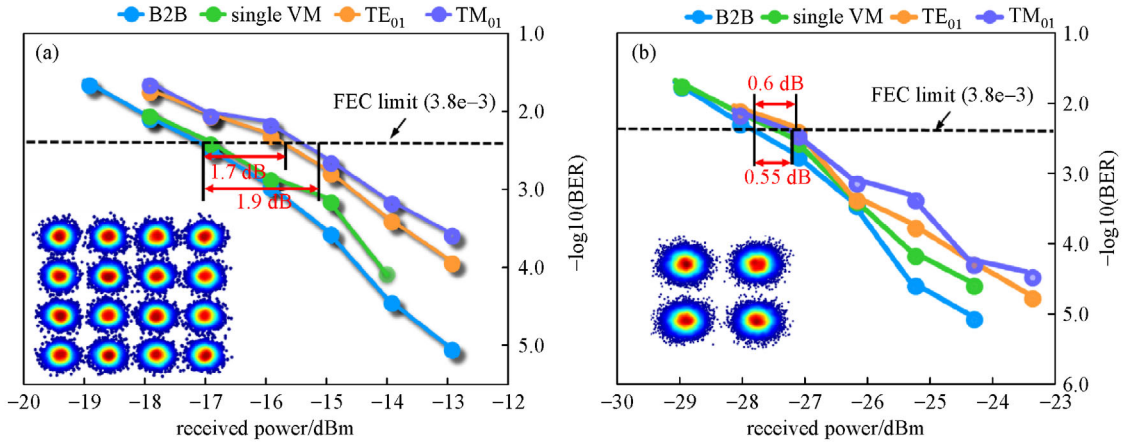

Fig. 15 BER performances of VMDM transmission over FMF link of length (a) 5 m with 16QAM; (b) 100 m with QPSK [23]

photo-detector at receiver as usual, and the yielded electrical signal is then sampled via real-time OSC and the off-line DSP is used to recovery the transmitted information.

Figure 15 shows the measured BER performance for the VMDM transmission over FMF. For 16QAM-OFDM signal transmission, it can be observed that there are 1.7, 1.9 dB power penalties between B2B and 5 m FMF respectively under the FEC threshold of 3.8×10^{-3}. However, for QPSK transmission, only 0.6 and 0.55 dB power penalties are observed after transmission over 100 m FMF. Meanwhile, the received power is much lower than that of 16QAM transmission.

5 Conclusion

In conclusion, the vector-mode-based mode division multiplexing transmission systems over free-space optical link and few-mode fiber have been reviewed. We use the commercial QP as the VM converter to realize the generation of cylindrical vector beams and then implement the MDM transmission over short-reach optical link. By using the DD-OFDM technology, we achieved the high-speed VMDM transmission without the MIMO digital signal processing. Thus, both the FSO and FMF experimental transmission results show that the VM-based MDM technique has the potential in optical interconnects such as datacenter or high-performance computing.

Acknowledgements This work was supported by the National High Technology 863 Research and Development of China (No. 2015AA017102), the National Natural Science Foundation of China (NSFC) (Grant Nos. 61575082, 61435006, 61525502, and 61490715), the Youth Science and Technology Innovation Talents of Guangdong (No. 2015TQ01X606), Guangdong Provincial Natural Science Foundation (GDSF) (No. 2015A030313328) and Pearl River S&T Nova Program of Guangzhou (No. 201710010051).

References

1. Kilper D, Bergman K, Chan V W S, Monga I, Porter G, Rauschenbach K. Optical networks come of age. Optics and Photonics News, 2014, 25(9): 50–57
2. Richardson D, Fini J, Nelson L. Space-division multiplexing in optical fibres. Nature Photonics, 2013, 7(5): 354–362
3. Winzer P. Spatial multiplexing in fiber optics: The 10 × scaling of metro/core capacities. Bell Labs Technical Journal, 2014, 19: 22–30
4. Li G, Bai N, Zhao N, Xia C. Space-division multiplexing: the next frontier in optical communication. Advances in Optics and Photonics, 2014, 6(4): 413–487
5. Fiorani M, Tornatore M, Chen J, Wosinska L, Mukherjee B. Spatial division multiplexing for high capacity optical interconnects in modular data centers. Journal of Optical Communications and Networking, 2017, 9(2): A143–A153
6. Franz B, Bülow H. Mode group division multiplexing in graded-index multimode fibers. Bell Labs Technical Journal, 2013, 18(3): 153–172
7. Benyahya K, Simonneau C, Ghazisaeidi A, Barre N, Jian P, Morizur J F, Labroille G, Bigot M, Sillard P, Provost J G, Debregeas H, Renaudier J, Charlet G. Multiterabit transmission over OM2 multimode fiber with wavelength and mode group multiplexing and direct detection. Journal of Lightwave Technology, 2018, 36(2): 355–360
8. Luo J, Li J, Sui Q, Li Z, Lu C. 40 Gb/s mode-division multiplexed DD-OFDM transmission over standard multi-mode fiber. IEEE Photonics Journal, 2016, 8(3): 7905207
9. Wen H, Xia C, Vel'azquez-Ben'ıtez A, Chand N, Antonio-Lopez J E, Huang B, Liu H, Zheng H, Sillard P, Liu X, Effenberger F, Amezcua-Correa R, Li G. First demonstration of six-mode PON achieving a record gain of 4 dB in upstream transmission loss budget. Journal of Lightwave Technology, 2016, 34(8): 1990–1996
10. Willner A, Huang H, Yan Y, Ren Y, Ahmed N, Xie G, Bao C, Li L, Cao Y, Zhao Z, Wang J, Lavery M P J, Tur M, Ramachandran S, Molisch A F, Ashrafi N, Ashrafi S. Optical communications using orbital angular momentum beams. Advances in Optics and Photonics, 2015, 7(1): 66–106

11. Lei T, Zhang M, Li Y, Jia P, Liu G N, Xu X, Li Z, Min C, Lin J, Yu C, Niu H, Yuan X. Massive individual orbital angular momentum channels for multiplexing enabled by Dammann gratings. Light, Science & Applications, 2015, 4(3): e257
12. Wang A, Zhu L, Wang L, Ai J, Chen S, Wang J. Directly using 8.8-km conventional multi-mode fiber for 6-mode orbital angular momentum multiplexing transmission. Optics Express, 2018, 26(8): 10038–10047
13. Milione G, Lavery M P, Huang H, Ren Y, Xie G, Nguyen T A, Karimi E, Marrucci L, Nolan D A, Alfano R R, Willner A E. 4 × 20 Gbit/s mode division multiplexing over free space using vector modes and a *q*-plate mode (de)multiplexer. Optics Letters, 2015, 40 (9): 1980–1983
14. Zhang J, Li F, Li J, Feng Y, Li Z. 120 Gbit/s 2× 2 vector-modes-division-multiplexing DD-OFDM-32QAM free-space transmission. IEEE Photonics Journal, 2016, 8(6): 7907008
15. Wang L, Nejad R M, Corsi A, Lin J, Messaddeq Y, Rusch L, LaRochelle S. Linearly polarized vector modes: enabling MIMO-free mode-division multiplexing. Optics Express, 2017, 25(10): 11736–11749
16. Rusch L A, Larochelle S. Fiber transmission demonstrations in vector mode space division multiplexing, Frontiers of Optoelectronics, 2018, 11(2): 155–162
17. Qiao W, Lei T, Wu Z, Gao S, Li Z, Yuan X. Approach to multiplexing fiber communication with cylindrical vector beams. Optics Letters, 2017, 42(13): 2579–2582
18. Liu J, Li S, Zhu L, Wang A D, Chen S, Klitis C, Du C, Mo Q, Sorel M, Yu S Y, Cai X L, Wang J. Direct fiber vector eigenmode multiplexing transmission seeded by integrated optical vortex emitters. Light, Science & Applications, 2018, 7(3): 17148
19. Milione G, Evans S, Nolan D A, Alfano R R. Higher order Pancharatnam-Berry phase and the angular momentum of light. Physical Review Letters, 2012, 108(19): 190401
20. Zhang J, Li F, Li J, Li Z. 95.16-Gb/s mode-division-multiplexing signal transmission in free-space enabled by effective-conversion of vector beams. IEEE Photonics Journal, 2017, 9(4): 1–9
21. Zhang J, Li F, Li J, Li Z. 228 Gb/s vector-mode-division-multiplexing signal transmission in free-space based on optical frequency comb. In: Proceedings of 2017 16th International Conference on Optical Communications and Networks (ICOCN). 2017, paper. 391
22. Ramachandran S, Kristensen P, Yan M F. Generation and propagation of radially polarized beams in optical fibers. Optics Letters, 2009, 34(16): 2525–2527
23. Li J, Zhang J, Li F, Huang X, Gao S, Li Z. DD-OFDM transmission over few-mode fiber based on direct vector mode multiplexing. Optics Express, 2018, 26(14): 18749–18757

Jianping Li received his B.S. degree in electronic science and technology from Jishou University in 2004, M.S. degree in communications and information system from South-west Jiaotong University in 2007 and Ph.D. degree in physical electronics from Beijing University of Posts and Telecommunication in 2012. And then he joined the Institute of Photonics and Technology at Jinan University as a lecturer. Since Oct. 2014, he has been promoted to an Associate professor in Institute of Photonics and Technology. Dr. Li has published/co-published more than 40 papers in top international journals and more than 20 conference papers (including invited talks). The main research interest of Dr. Li is focused on high-speed fiber communication system including optical frequency comb generation, mode division multiplexing and short-reach optical interconnect, etc.

Zhaohui Li obtained his B.S. degree in the Department of Physics and M.Sc. degree in the Institute of Modern Optics from Nankai University, China in 1999 and 2002 respectively, and his Ph.D. degree from the Nanyang Technological University 2007. Now, he is working in the School of Electronics and Information Technology, Sun Yat-sen University, China, as professor in 2009. His research interests are optical communication systems, optical signal processing technology and ultrafine measurement systems.